Lawrence Berkeley National Laboratory
Recent Work

Title
RADIATION DAMAGE STUDIES BY X-RAY PHOTO-ELECTRON SPECTROSCOPY: III. ELECTRON IRRADIATED HALATES AND PERHALATES

Permalink
https://escholarship.org/uc/item/0cf8g96z

Author
Sasaki, T.

Publication Date
1979-07-01

⌷⌷ Lawrence Berkeley Laboratory
UNIVERSITY OF CALIFORNIA, BERKELEY, CA

Materials & Molecular Research Division

RADIATION DAMAGE STUDIES BY X-RAY PHOTOELECTRON
SPECTROSCOPY: III. ELECTRON IRRADIATED HALATES
AND PERHALATES

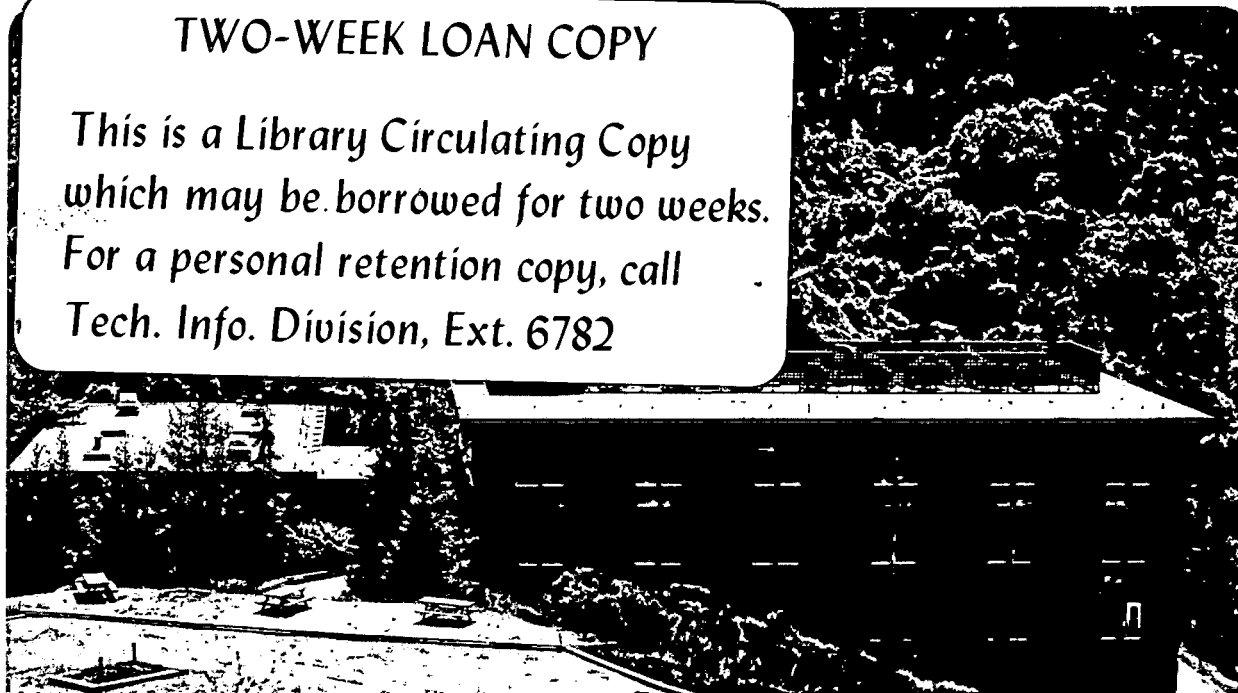T. Sasaki, R. S. Williams, J. S. Wong, and D. A. Shirley

July 1979

DISCLAIMER

LBL-7399

RADIATION DAMAGE STUDIES BY X-RAY PHOTOELECTRON SPECTROSCOPY:
III.   ELECTRON IRRADIATED HALATES AND PERHALATES*

T. Sasaki,‡ R. S. Williams,‡ J. S. Wong, and D. A. Shirley

Materials and Molecular Research Division
Lawrence Berkeley Laboratory
and
Department of Chemistry
University of California
Berkeley, California 94720

July 1979

ABSTRACT

X-ray photoelectron spectroscopy (XPS) ·was employed to identify radiolytic products in $NaClO_3$, $LiClO_4$, $LiBrO_3$, and $LiIO_4$, which were irradiated in situ with 1.4 keV electrons. While $LiIO_4$ was exceedingly resistant to radiation damage, the remaining compounds decomposed readily by an apparent stepwise release of oxygen from the parent oxyanion to form XO_3^-, XO_2^-, X^- (X = Cl or Br) and O_2. Heavy irradiation produced IO_3^- in $LiIO_4$ and alkali halide, and alkali-metal oxide in the remaining compounds. These final products were cathodochromic, with both trapped electron (F or anion vacancy) and hole (V_k or X_2^-) centers being formed. Photobleaching of these centers also induced a partial reoxidation of the halogen species that had been formed by radiation-induced reduction. Comparison of the production rate of Li_2O with that of $X_2^- + X^-$ suggests that Li_2O is not a primary product, but may be produced via oxidation of colloidal particles of metallic lithium in the alkali halide layer of the heavily irradiated samples.

I. INTRODUCTION

Numerous studies of radiolysis have been carried out to determine chemical distributions of products in crystalline alkali-metal halates and perhalates exposed to such ionizing radiations as ^{60}Co gamma-rays and soft X-rays. Using quantitative chemical analyses, Boyd and Brown[1,2] observed ClO_4^-, ClO_2^-, ClO^-, Cl^-, O_2^-, O_3^-, and probably ClO_2 produced in $KClO_3$ on irradiation with ^{60}Co gamma-rays at room temperature. The dominant product (formed with a G value of 2.06) was found to be ClO_2^-. On the other hand, ESR spectroscopy of irradiated $KClO_3$ indicated the formation of five paramagnetic species: ClO_2, O_3^-, and $(Cl-ClO_2)^-$ at room temperature[3] and ClO_3 and ClO_3^{2-} at low temperatures.[4,5] Similar chemical species have been observed at room temperature for irradiated $KBrO_3$,[6] with such stabilized radicals as $(BrO-BrO_3)^-$, BrO_3^{2-} and O_2^- observed[7] instead of ClO_2 and $(Cl-ClO_2)^-$ in irradiated $KClO_3$. Mechanisms for the formation of these products have been proposed by Zakharov and Nevostruev[8] and also by Boyd and Brown.[2]

The halogens have several stable oxidation states both as solid salts and in solution. As indicated above, several of these states are evidently produced in the radiolysis of halates and perhalates. A universal method for detecting these products would be quite valuable. X-ray photoelectron spectroscopy (XPS) shows promise in this regard. It is very sensitive to changes in oxidation state and is therefore a powerful technique for the determination of the chemical states of radiolytical products. The XPS technique is also advantageous in allowing direct _in situ_ observation of the species trapped within the crystal lattice, and it is sensitive to molecular species undetectable by ESR.

a commonly-used technique for analyzing the chemical products of radiolysis.

Prins[9] has found radiolytical products such as ClO_3^-, ClO^-, and Cl^- on a $NaClO_2$ sample exposed to Al Kα X-rays during XPS measurements. Stimulated by his findings and our previous radiation damage studies,[10,11] we applied XPS to the examination of chemical changes in the oxygen ligand as well as the central halogen in electron-irradiated $NaClO_3$, $LiClO_4$, $LiBrO_3$, and $LiIO_4$. In this paper, the radiolytical products identified in the electron-irradiated solids are compared with observations for gamma-ray radiolysis by other workers. It is found that, except in the case of $LiIO_4$, reduction of the halogen is accompanied by stepwise release of oxygen from the parent oxyanion and that heavy irradiations result in the formation of X^-, O_2, and alkali metal oxide. Intense color center formation due to electron bombardment is observed, and the existence of a trapped hole center X_2^- is inferred from the data.

II. EXPERIMENTAL

A single crystal of $LiClO_4$ was grown by slow cooling of its melt. $LiBrO_3$ and $LiIO_4$ powders were pressed into pellets 6mm in diameter, using a pressure of 120 kg/cm^2. The samples were stored in a vacuum desiccator until the XPS measurements because they are highly hygroscopic.

The experimental apparatus and procedures used for electron irradiation of the samples and subsequent XPS measurements have been described in detail elsewhere.[10] Because of the extreme sensitivity of the $NaClO_3$, $LiClO_4$, and $LiBrO_3$ even to Al Kα X-rays, the sampling

position of the crystal surfaces was varied slightly every five hours during the ca. 15-hour XPS measurement of the valence band. After heavy irradiation with 1.4 keV electrons some samples had turned deep blue due to the formation of color centers. Photobleaching was performed by shining a 200 W tungsten filament lamp through a quartz window. While the base pressure of the spectrometer was less than 1×10^{-9} Torr, the pressure increased slightly during the photobleach procedure, which required about 2 hours to bleach the samples completely. Both during and after the experiments, carbon contamination of the sample surface was below detection limits.

Any change in the Fermi level caused by electron irradiation was not detectable using XPS; no shifts in a given core-level energy of the same chemical state were observed despite the changes in the chemical composition of the sample surface. All binding energies, if not otherwise noted, were referenced against the edge of the valence band for the respective alkali halide which was the main final product of the radiolysis. All other procedures in this experiment were the same as previously described.[10]

III. RESULTS AND ANALYSES

A. Spectral Changes and Product Identification in Irradiated $NaClO_3$.

All the observed peak binding energies, including molecular orbital energies, for the compounds investigated are compiled in Tables I and II.

The $NaClO_3$ sample was very sensitive to irradiation. Figure 1(a) shows the Cl(2p) region before irradiation. A small amount of reduced chlorine attributable to Cl^- is observed near 199 eV binding energy (E_B). This is due to radiolysis caused by Al Kα X-rays during the

XPS measurements.[12-14] Electron bombardment caused vast changes in the core-level region so quickly that intermediate stages of product formation by radiolysis were not observable. Figure 1(b) shows the core-level shift caused by a ten-second low-level radiation dose. No peaks attributable to chlorine oxyanions are observed. The incident charge, calibrated by using a Faraday cup, is given in the rectangles in units of Coulomb/cm^2. Even after heavy irradiation (0.3 C/cm^2 of 1.4 keV electrons) the spectral shape remained essentially unchanged, as seen in Fig. 1(c). Assuming equal line widths for all chemical species, a spectral fitting analysis using Gaussian peaks suggests the presence of three chemically different chlorine species in the spectral feature of Fig. 1(b). The main product B is assigned as Cl^- from its chemical shift given in Table II and from spectral changes in the valence band region (to be shown in Fig. 3). The apparent broadening to lower binding energy, represented as peak C, may indicate the presence of inequivalent binding sites for Cl^- anions in the chemically altered lattice, or may simply be an artifact of the procedure used to fit the spectra. However, the feature denoted peak A represents a definite chemical species of Cl which appears to be in an oxidation state between Cl^- and ClO^-. In addition, the sample surface developed a faint blue coloration, indicating the presence of color centers.

Exposure of the sample to white light from a tungsten lamp removed the faint blue coloration, revealing a cloudy surface. The resultant XPS spectrum is shown in Fig. 1(d). The most significant change in the spectrum is the reappearance of a small amount of the parent chlorine species. Also significant is the disappearance of the high binding

energy broadening of the main Cl$^-$ 2p spectral feature, i.e., there is

strong attenuation of peak A. This observation may be interpreted by

assigning peak A to the species Cl$_2^-$, as the chemical identity of a trapped

hole or V$_k$ center in an alkali chloride lattice. Other investigations

have shown that V$_k$ centers are stable in alkali halide lattices only

at low temperatures,[15] but are stable in irradiated KClO$_3$[3] and

Ca(ClO$_3$)$_2$·H$_2$O at room temperature.[16]

The spectral changes in the O(1s) region which result from e$^-$

irradiation and subsequent photobleaching are shown in Fig. 2. Three

new peaks—D, E, and F—at energies different from the parent O(1s)

peak position are required to obtain good fits to the spectra of

Figs. 2(b) and (c). The assignment of these peaks to chemical species

is somewhat confused by the presence of a product peak at the same

energy as the O(1s) line from ClO$_3^-$, even though the Cl(2p) spectra in

Fig. 1(b) show no evidence of a signal from the parent (i.e., not

reduced) species. This has been pointed out by Copperthwaite and

Lloyd,[12-14] who observed a peak corresponding to D and a peak at the

same energy as O(1s) in ClO$_3^-$ in soft X-ray irradiated NaClO$_3$; the latter

they assigned to O$_2^-$ trapped in a lattice site of the crystal and the

former to interstitial O atoms associated with O$_2^-$ in a complex similar

to ozonide ion.

Our data on e$^-$ irradiated NaClO$_3$ presented in Fig. 1(b) are not

consistent with this interpretation, because D has roughly twice the

intensity of the residual peak at the parent binding energy. We assigned

peak D as due to O(1s) photoemission from molecular O$_2$ trapped in the

solid. An O$_2$ peak should be detectable because of the high G-value

(2.36) for its production observed by Burchill et al.[17] for powdered

$NaClO_3$. Peak F is readily assigned to the $O(1s)$ line of Na_2O (by

analogy with $O(1s)$ of Li_2O in irradiated $LiClO_4$ and $LiBrO_3$ described

later). The assignments of feature E and the residual peak at the parent

binding energy are open questions, although a strong candidate for one

of these peaks is O_3^-. The formation of O_3^- in gamma-irradiated $NaClO_3$

and $KClO_3$ single crystals has been well-established by ESR,[3] resonance

Raman,[18] and optical[2,19,20] spectroscopies. A similar $O(1s)$ line was

observed in irradiated Li_2SO_4 and $LiNO_3$ and attributed to O_3^-.[10] The

apparent high intensity of the $O(1s)$ line of the residual peak in

Fig. 2(b) is due to the scale normalization used for the figure. Its

actual peak intensity relative to the $O(1s)$ of ClO_3^- in Fig. 2(a) is

approximately 0.14, which agrees with observations of X-ray irradiated

$NaClO_3$.[12] The photobleach produced the spectrum shown in Fig. 2(c).

A notable change is the apparent regeneration of the parent species,

as was observed in Fig. 1(d).

In Fig. 3(a), we show the valence band region, including the $Na(2s)$

and $Na(2p)$ lines, of the preirradiated $NaClO_3$. Although the $1a_1$ orbital

peak overlaps the $Na(2p)$ peak, the spectral pattern is almost the same

as that for $LiClO_3$ in a recent publication by Calabrese and Hayes.[21]

From the core-level shift in Fig. 1(c), peaks (II) and (III) in the

spectra of the irradiated sample (Fig. 3(b)) are assigned as the $Cl(3s)$

and $Cl(3p)$ lines, respectively. The shoulder on the high-energy side

of the $Cl(3p)$ line was discussed previously[22] and ascribed to splitting

of the valence-band structure in NaCl. The weakest—peak (I)—is

attributed to the $O(2s)$ lines of the species which give rise to peaks D,

E, and F, and the residual feature in Fig. 2(b). The FWHM of the Na(2s) line increased from 1.7 eV in Fig. 3(a) to 2.5 eV in Fig. 3(c), probably because of the existence of at least two chemically different Na^+ ions contributing to the latter spectrum.

B. Spectral Changes and Product Identification in Irradiated $LiClO_4$

Long-term exposure of the $LiClO_4$ crystal to Al $K\alpha$ X-rays caused a pronounced change in the core-level peaks. Fig. 4 demonstrates the effect of X-ray exposure on the Cl(2p) region. A new photopeak, indicated as G, appeared after exposure to source X-rays for 24 hours. The labels H and J refer to the expected positions of further reduction products. Radiation products were identified from their chemical shifts, given in the third column of Table II. In spite of the distinct changes in the core-level peaks, the valence-band region remained unchanged regardless of exposure time. This is compatible with the observation that the valence band spectrum of ClO_3^-, which is the dominant product formed by X-ray exposure, is very similar to that of ClO_4^-. [23,24] Electron irradiation brought about further, more drastic changes in the core-level regions. Fig. 5(a) was obtained for a sample that was subjected to the same X-ray exposure history as that of Fig. 4(a) and subsequent electron irradiation for 15 seconds. Deconvolution analyses indicated the possibility of a small contribution of an additional peak I on the high binding energy side of peak J. This peak I corresponds closely in energy to the product peak A, ascribed to Cl_2^-, observed in Fig. 1. Continued irradiation revealed that ClO_3^- and ClO_2^- as well as ClO_4^- are further reduced to Cl^- and Cl_2^-, as shown in Fig. 5(b). The

accumulation of Cl_2^- in the surface layer is supported by a distortion toward the high binding energy side of the main photopeak in Fig. 5(b). Whereas irradiation of the $NaClO_3$ sample produced a broadening of the Cl^- peak to lower E_B represented by C in Fig. 1(b), no corresponding broadening was found for irradiated $LiClO_4$.

Electron bombardment also produced a deep blue coloration of the sample surface, which is evidence of color-center formation. Spectra obtained after photobleaching the colored sample revealed the reformation of ClO_2^-, ClO_3^-, and ClO_4^-, as seen in Fig. 5(c). The decoloration was also accompanied by removal of the high binding energy distortion of the main product peak, indicating the disappearance of Cl_2^-. These phenomena are analogous to those reported for $NaClO_3$.

Spectral changes in the O(1s) region are shown in Fig. 6. The measured maximum spectral intensities of Figs. 6(b), 6(c), and 6(d) relative to that of Fig. 6(a) were 0.37, 0.20, and 0.63, respectively. Irradiation resulted in decreases in the O(1s) intensity of ClO_4^- and the gradual appearance of new photopeaks. Fig. 6(b) was unfolded into four Gaussians whose widths were taken to be that of Fig. 6(a). The smallest peak in the fit is at the energy position of the parent species. Peaks K and L are assigned as the O(1s) lines of ClO_3^- and ClO_2^-, respectively, because the O(1s) energy is expected to decrease in the order of $ClO_4^- > ClO_3^- > ClO_2^-$. On the other hand, peak M, which must arise from a highly polarized species, is assigned to the O(1s) line of Li_2O.[10] Since the heaviest irradiation (0.46 C/cm^2 of 1.4 keV electrons) resulted in spectral features essentially identical to Fig. 6(c), Li_2O is clearly a fairly stable product of irradiated $LiClO_4$. The O(1s)

region of Fig. 6(d) showed striking evidence that photobleaching is accompanied by oxidation of the lower-oxidation-number halogen species. Analysis of the peak intensities shows that the relative amounts of the species reformed are qualitatively consistent with those of Fig.5(c).

Spectral features in the valence-band region are displayed in Fig. 7. Photopeaks from molecular orbitals of ClO_4^- given in Fig. 7(a) were completely replaced by the new peaks (IV), (V), and (VI) after irradiation to 0.46 C/cm^2, as seen in Fig. 7(b). Since the Cl(2p) region in Fig. 5(b) indicated essentially complete reduction to Cl^- and Cl_2^-, peaks (V) and (VI) are assigned as the Cl(3s) and Cl(3p) lines of these species, respectively. The intensity of peak (V) relative to that of peak (VI) and the shape of peak (VI) characterized by a small shoulder on the high binding energy side are the same as those observed for NaCl[22] and LiCl.[25] Peak (IV), on the other hand, is due mainly to the O(2s) line of Li_2O. This peak may contain slight contributions from the $^2S(3s^2 3p^4 3d)$ and $^2S(3s^2 3p^4 4d)$ states of Cl^- (ground state: $^1S(3s^2 3p^6)$), as suggested by Prins.[25] The peak assignments of the valence-band region are compatible with the chemical shift of the Li(1s) line toward the low binding energy side in Fig. 7(b), where the higher-energy peak arises primarily from LiCl while the lower-energy contribution is from Li_2O. Photobleaching of the colored sample yielded the spectrum shown in Fig. 7(c). The reformation of ClO_4^-, ClO_3^-, and ClO_2^-, which have similar valence band spectra, is again suggested.

C. Spectral Changes and Product Identification in Irradiated $LiBrO_3$

The $LiBrO_3$ sample was also very sensitive to irradiation. Fig. 8(b) shows the Br(3p) region of the sample after irradiation for five seconds. The spectrum reveals the presence of bromine in four different oxidation states. A computer fit using four spin-orbit doublets with the relative intensities and FWHM of the doublet peaks determined from Fig. 8(a) is indicated by dashed lines. The $Br(3p_{3/2})$ and Br(3d) energies for the different chemical species as determined by the peak fitting scheme are included in Table II with some related data. From the chemical shifts, the products are assigned as BrO_2^-, BrO^-, and Br^-. The formation of the same species has been pointed out by Boyd and co-workers[2,6,26] for crystalline alkali bromates exposed to ^{60}Co gamma-rays with relatively high yields for BrO_2^-, Br^-, and also O_2. The entire XPS spectrum gradually shifted to lower binding energy with increasing irradiation time. Heavy irradiation turned the sample surface deep blue. The color was different from the light-yellow to gold (assigned to O_3^- formation[6]) reported for gamma-irradiated $LiBrO_3$. The blue coloration implies formation of color centers in the surface layer of LiBr formed on the irradiated $LiBrO_3$. No clear evidence was obtained for the formation of Br_2^- as a counterpart of the trapped electron centers as in the case for Cl_2^- in heavily irradiated $NaClO_3$ and $LiClO_4$.

Photobleaching the colored sample resulted in the reappearance of photopeaks corresponding to BrO_3^- and BrO_2^-, as shown in Fig. 8(d). Although the presence of Br_2^- was not confirmed in Fig. 8(c), processes for the oxidation of bromine initiated with the photobleaching may be similar to that of chlorine in the irradiated $NaClO_3$ and $LiClO_4$, as

discussed later. Both the Br(3s) and Br(3d) regions revealed the same chemical changes as those of the Br(3p) region.

After irradiation, new O(1s) peaks—Q and R (originating from BrO_2^- and Li_2O, respectively)—appeared. The assignment of peak R is supported by the fact that it slowly increased in relative intensity and survived heavy irradiation, as seen in Fig. 9(b). Fig. 9(b) does not show strong evidence for the formation of O_3^-, which has been observed for gamma-irradiated $NaBrO_3$,[27-29] $KBrO_3$,[30] and $CsBrO_3$.[1] In Fig. 9(c) the reformation of the parent species during photobleaching of the color center is again observed.

The valence-band spectrum taken with careful variation of the electron collection position to minimize the impact of X-radiation damage on the spectrum is given in Fig. 10(a). We noted the energy resolution of this spectrum is better than that in a recent publication by Nefedov et al.[24] Electron irradiation caused a gradual decrease in the intensity of the molecular orbitals, producing the spectrum shown in Fig. 10(b), which is dominated by three new peaks and reveals a splitting of the Li(1s) line. Peak (VIII) is assigned to the Br(4s) line from Br^-, which is the dominant species as determined from Fig. 8(c). Peak (IX) is composed of the Br(4p) of Br^- and the O(2p) line of Li_2O. This photopeak is characterized by two shoulders on the high binding-energy side. One of them originates from the O(2p) line and the other is interpreted in terms of the band structure of $LiBr$,[22] which is a main final product on the sample surface. On the other hand, peak (VII) is mainly the O(2s) line of Li_2O. The photobleaching of the deeply colored sample yielded a spectrum analogous to those for the $NaClO_3$ and $LiClO_4$

samples, as shown in Fig. 10(c). In addition, the Li(1s) region was broadened by the presence of $LiBrO_3$, while Fig. 10(b) shows a sharp separation due to the Li(1s) lines of LiBr and Li_2O at the high and low energy sides, respectively.

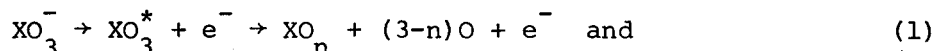## D. Identification of the Products in Irradiated $LiIO_4$

In contrast to the preceding examples, $LiIO_4$ was very resistant to irradiation, as observed previously.[2] There was no apparent change in color of the irradiated sample surface. However, heavy irradiation of 0.49 C/cm^2 of 1.4 keV electrons caused decreases in the $I(3d_{5/2})$ and O(1s) binding energies by 0.8 and 1.0 eV, respectively. The core-level energies of the product are given in Table I. From the chemical shift in the $I(3d_{5/2})$ energy, the product is assigned as IO_3^-. The $I(3d_{5/2})$ energy of IO_3^- has been found to be lower by 1.5 eV than that of IO_4^-.[31] There was no photopeak attributable to further radiolytical products such as I_2 and I_3^- which have been observed for gamma-irradiated $LiIO_3$.[32] Also, there was no evidence for the occurrence of the alkali-metal oxide found in the preceding samples. These results are in general agreement with observations for gamma-irradiated KIO_4.[2]

IV. DISCUSSION

The study of radiation damage due to low-energy electrons is quite important, because any ionizing radiation in a solid creates a cascade of electrons. Hot electrons dissipate energy via the creation of electron-hole pairs in the electron-irradiated halates and perhalates; the nonradiative decay of these localized excited states can lead to drastic changes in the chemistry of a solid.

Some of the electron and hole states formed can be trapped at defect sites formed in the altered lattice structure. Good candidates for these trapping sites are vacant anion sites for electrons (F and assorted centers), producing a visible coloration of the sample, and V_k centers (X_2^-) for holes. These centers are bleachable by a white light source. In conjunction with bleaching, regeneration of oxyanion species is observed. The oxidant responsible for this reformation of higher oxidation state species may well be the trapped hole centers, X_2^-, which react with alkali oxides to generate halates or perhalates. Further study is required to elucidate the reaction(s) responsible for this light-induced oxidation process; studies of low-energy electron irradiation with XPS and perhaps optical reflectance spectroscopies at various temperatures should prove to be quite interesting.

Heavy electron irradiation of chlorine and bromine oxyanions yielded alkali halides, alkali-metal oxides, and molecular oxygen as the main chemical products. Although not observed in our study, the formation of XO_4^- has been observed in gamma-irradiated halates such as $KClO_3$[1,17] and $CsBrO_3$[2,33] with fairly high G values (0.96-1.13 and ca. 0.7, respectively). Both Heal[34] and Boyd and Brown[2] have postulated perhalate formation via addition of oxygen to the matrix molecule. The primary steps of the radiolysis are assumed to be the ionization and excitation of XO_3^-. Possible mechanisms for the scission of an X-O bond are

$$XO_3^- \rightarrow XO_3^* + e^- \rightarrow XO_n + (3-n)O + e^- \quad \text{and} \qquad (1)$$

$$XO_3^- \rightarrow XO_3^{-*} \rightarrow XO_2^- + O. \qquad (2)$$

Oxygen atoms produced via reactions (1) and (2) may lead to abstraction, addition, or direct combination of the atoms:

$$O + XO_3^- \rightarrow XO_2^- + O_2, \tag{3}$$

$$O + XO_3^- \rightarrow XO_4^-, \quad \text{and} \tag{4}$$

$$O + O \rightarrow O_2. \tag{5}$$

Whereas the reaction rates (3) and (4) are first-order in oxygen concentration, that for reaction (5) is second-order. For this reason, reaction (5) should be favored in radiolysis with high linear energy transfer (LET) radiations, such as energetic electrons and ions. The LET of 1.4 keV electrons employed in the present work is estimated to be about 2 eV/$\overset{\circ}{A}$, more than 30 times that of ^{60}Co gamma-rays and soft X-rays. Accordingly, the competitive reactions (3) and (4) are suppressed, resulting in the absence of perhalate species in the irradiated $NaClO_3$ and $LiBrO_3$ samples.

On the other hand, products from reactions (1) and (2) could undergo successive radiolysis due to their large concentration on the sample surface. Chemical decomposition of the heavily-irradiated surface produces a thin layer of alkali halide containing various types of structural defects. It is well-known that exposure of alkali halides to ionizing radiations, including energetic electrons, efficiently produces F-centers; i.e., trapped electrons in vacant halogen sites. However, the blue coloration of the present samples, which are assumed to have absorption maxima around 6000 $\overset{\circ}{A}$, is different from that expected for F-centers[35] in NaCl, LiCl, and LiBr. This discrepancy may arise from the distorted lattice structures of the alkali halides produced

on the sample surfaces. The degree of lattice expansion may be estimated
from the Ivey-Mollwo relation,[36]

$$\lambda_{max}(\text{Å}) = 703 \times d^{1.84} \tag{6}$$

which relates the maximum in the F-center absorption spectrum λ_{max}
to d, the interionic distance in Ångstroms. This predicts a ca. 1 Å
increase in the interatomic distance of the observed radiation products
relative to the normal alkali halide lattice spacing. Whereas the Na-Cl
and Li-Cl distances in the alkali halides are 2.81 and 2.57 Å, respec-
tively, those in $NaClO_3$ and $LiClO_4$ are 4.00 and 4.64 Å as determined
from their lattice structures.[37] Thus, the electronic states which
cause the blue coloration of our samples might arise from color centers
in a highly perturbed alkali halide lattice. It is also reasonable that
structural expansion can facilitate reformation of the original material
as was observed in the photobleaching experiment. No photopeaks attrib-
utable to the trapped electron centers were found, due both to the low
color-center concentration and its small photoionization cross-section
at Al Kα X-ray energies. The absolute photoemission cross-section of
a color center should be roughly the same order of magnitude as atomic
hydrogen, which is estimated to be 10^{-3} that of the Cl(3p) shell.[38]

The discovery of alkali-metal oxide formation is quite important,
since the chemical fate of the positive ion in the radiolysis of the
halates and perhalates is largely unknown. Fig. 11 shows the changes
in the amounts of $(X_2^- + X^-)$ and Li_2O in the $LiClO_4$ and $LiBrO_3$ samples.
It is clear that in both cases the formation of Li_2O does not begin
until more than 60% of the original material is converted into the

alkali halide. This strongly suggests that Li_2O is not a primary product but is produced in a secondary reaction, perhaps via oxidation of colloidal particles of lithium. Aggregation of alkali-metal particles by electron irradiation has been found in such alkali halides as LiF,[39,40] NaCl,[39,41] KCl,[39,40] and KBr.[41] The oxygen for the oxidation of the colloidal particles is produced via reactions such as Eqs. (1) and (2). This is supported by the observation of O_2 formed during X-ray irradiation of $NaClO_3$.[12] The relative amounts of lithium stabilized as the oxide in the heavily irradiated $LiClO_4$ and $LiBrO_3$ were estimated from Figs. 7(b) and 10(b) to be about 35 and 50%, respectively.

The exceptional stability of $LiIO_4$ to electron radiation may be due to the fact that the radiative lifetimes of the excited electronic states induced by electron bombardment are shorter than nonradiative decay mechanisms, whereas the opposite is true for the $NaClO_3$, $LiClO_4$, and $LiBrO_3$. Thus, the excessive energy deposited into the crystal lattice by electron irradiation may be reradiated as photons. Such radiation should be detectable during electron bombardment and could help to identify the particular electronic states excited.

V. CONCLUSION

Through this series of radiation damage studies, XPS has proved to be a very useful technique for the detection of radiolytical products on solid surfaces. After irradiation of various crystalline oxyanions with 0.3-1.6 keV electrons, both the oxidation states of the central atom and some of the chemical states of oxygen and alkali-metal were determined.

As for the halates and perhalates, excluding $LiIO_4$, the major

products in the initial stage of the radiolysis were identified as

XO_3^-, XO_2^-, X^-, and O_2^-, almost the same as those observed in gamma-

irradiation. The major difference is the absence of XO_4^- after electron

irradiation. This difference is interpreted in terms of the difference

in the LET of the two radiations and the concentrations of oxygen

produced. Further radiolysis led to stepwise release of oxygen; i.e.,

reduction of the central halogen atom, finally resulting in the formation

of alkali halide and alkali-metal oxide as the stable solid-phase

products. This mixture proved to be cathodochromic; i.e., electron

irradiation produced color centers that were bleachable. Both electron

centers (F-center and/or related species) and hole (V_k or X_2^-) centers

were produced in $NaClO_3$, $LiClO_4$, and $LiBrO_3$ samples. It is also

suggested that the alkali-metal oxide is not a primary product but is

produced via the oxidation of colloidal particles of the alkali-metal

formed in the radiation damage layer.

Footnotes and References

‡Present address: Chemistry Division, Japan Atomic Energy Research Institute, Tokai-Mura, Ibaraki-ken 319-11, Japan.

‡Present address: Bell Laboratories, 600 Mountain Avenue, Murray Hill, New Jersey 07974.

[1] L. C. Brown and G.E. Boyd, J. Phys. Chem. 73, 396 (1969).

[2] G. E. Boyd and L. C. Brown, J. Phys. Chem. 74, 3490 (1970).

[3] R. S. Eachus, P. R. Edwards, S. Subramanian, and M.C.R. Symons, J. Chem. Soc. A, 1704 (1968).

[4] J.-C. Fayet, C. Pariset, and B. Thieblemont, Compt. Rend. Acad. Sci. (Paris) B 268, 78 (1969).

[5] R. S. Eachus and M. C. R. Symons, J. Chem. Soc. A, 2433 (1968).

[6] G. E. Boyd, E. W. Graham, and Q. V. Larson, J. Phys. Chem. 66, 300 (1962).

[7] T. Andersen, H. E. Lundager-Madsen, and K. Olesen, Trans. Faraday Soc. 62, 2409 (1966).

[8] Yu A. Zakharov and V. A. Nevostruev, Russ. Chem. Rev. 37, 61 (1968).

[9] R. Prins, J. Chem. Phys. 61, 2580 (1974).

[10] T. Sasaki, R. S. Williams, J. S. Wong, and D. A. Shirley, J. Chem. Phys. 68, 2718 (1978).

[11] T. Sasaki, R. S. Williams, J. S. Wong, and D. A. Shirley, J. Chem. Phys. 69, 4374 (1978).

[12] R. G. Copperthwaite and J. Lloyd, J.C.S. Dalton 11, 1117 (1977).

[13] R. G. Copperthwaite and J. Lloyd, J.C.S. Faraday I **74**, 2252 (1978).

[14] R. G. Copperthwaite and J. Lloyd, Nature **271**, 141 (1978).

[15] T. G. Castner and W. Känzig, J. Phys. Chem. Sol. **3**, 178 (1957).

[16] D. Suryanarayana and J. Sohanadri, J. Mag. Res. **16**, 274 (1974).

[17] C. E. Burchill, P. E. Patrick, and K. J. McCallum, J. Phys. Chem. **71**, 4560 (1967).

[18] J. B. Bates and J. C. Pigg, J. Chem. Phys. **62**, 4227 (1975).

[19] J. B. Bates and H. D. Stidham, Chem. Phys. Lett. **37**, 25 (1976).

[20] C. Ramasastry and S.B.S. Sastry, J. Phys. Chem. Sol. **29**, 399 (1968).

[21] A. Calabrese and R. G. Hayes, J. Electron Spectrosc. **6**, 1 (1975).

[22] S. P. Kowalczyk, F. R. McFeely, L. Ley, R. A. Pollak, and D. A. Shirley, Phys. Rev. B **9**, 3573 (1974).

[23] J. A. Connor, I. H. Hillier, V. R. Saunders, and M. Barber, Mol. Phys. **23**, 81 (1972).

[24] V. I. Nefedov, Yu V. Buslaev, N. P. Sergushin, Yu V. Kokurov, and V. V. Kovalev, J. Electron Spectrosc. **6**, 221 (1975).

[25] R. Prins, Chem. Phys. Lett. **19**, 355 (1973).

[26] G. E. Boyd and Q. V. Larson, J. Phys. Chem. **69**, 1413 (1965).

[27] T. Andersen, J. R. Byberg, and K. J. Olsen, J. Phys. Chem. **71**, 4129 (1967).

[28] F. T. Gamble, J. Chem. Phys. **47**, 1193 (1967).

[29] M. M. Cosgrove and M. A. Collins, J. Chem. Phys. **52**, 989 (1970).

[30] A. Begum, S. Subramanian, and M.C.R. Symons, J. Chem. Soc. A, 918 (1970).

[31] C. S. Fadley, S.B.M. Hagstrom, M. P. Klein, and D. A. Shirley, J. Chem Phys. **48**, 3779 (1968).

[32] K. Hasegawa, Nippon Kagaku Zasshi $\underline{90}$, 135 (1969).

[33] L. C. Brown, G.M. Begun, and G. E. Boyd, J. Amer. Chem. Soc. $\underline{91}$, 2250 (1969).

[34] H. G. Heal, Can. J. Chem. $\underline{37}$, 979 (1959).

[35] Optical absorption maxima of the F-centers in pure crystals of NaCl, LiCl, and LiBr have been known to be around 4700, 3850, and 4520Å, respectively. W. B. Fowler, Physics of Color Centers (Academic Press, New York, 1968).

[36] H. F. Ivey, Phys. Rev. $\underline{72}$, 341 (1947); C. P. Flynn, Point Defects and Diffusion (Oxford Univ. Press, London, 1972) p. 563.

[37] R.W.G. Wyckoff, Crystal Structures, Vol. 3 (Interscience Publishers, 1960).

[38] J. H. Scofield, J. Electron Spectrosc. $\underline{8}$, 129 (1976).

[39] G. C. Fryberg and R. A. Lad, Surf. Sci. $\underline{48}$, 353 (1975).

[40] L.S.C. Araiza and B. D. Powell, Surf. Sci. $\underline{51}$, 504 (1975).

[41] Y. A. Ekmanis and E. A. Rosauer, J. Appl. Phys. $\underline{46}$, 2837 (1975).

TABLE I. The binding energies (eV) of the core levels and valence-band region before and after electron irradiation.

| Orbital | NaClO$_3$ [a] | | Orbital | LiClO$_4$ [a] | |
	Before	After		Before	After
O(1s)	531.0	535.6(D)	O(1s)	533.9	533.6(K)
		533.2(E)			531.9(L)
		526.7(F)			529.1(M)
Cl(2s)	278.2		Cl(2s)	280.2	270.4
Cl($2p_{3/2}$)	207.3	~198.9	Cl($2p_{3/2}$)	209.5	~199.6
Na(2s)	62.0	61.8	Li(1s)	56.5	55.6
Na(2p)	30.0	29.6			53.2
$1a_1$	~29.0	21.4(I)	$4a_1$	33.6	22.7(IV)
3e	24.0		$3t_2$	26.3	
$6a_1$	14.3	15.4(II)	$5a_1$	16.0	15.8(V)
$2e_1$, $3a_1$	10.9		$4t_2$	12.9	
6e	6.9	4.4(III)	1e, $5t_2$	8.6	5.0(VI)
$8a_1$	4.6		$1t_1$	5.7	

| Orbital | LiBrO$_3$ [a] | | Orbital | LiIO$_4$ [b] | |
	Before	After		Before	After
O(1s)	533.2	531.7(Q)	O(1s)	529.5	528.5
		530.0(R)	I($3d_{5/2}$)	622.9	622.1
Br(3s)	264.7	~260.6	I(4p)	126.5	
Br($3p_{1/2}$)	197.3	~190.6	I(4d)	53.4	
Br($3p_{3/2}$)	190.9	~184.1	Li(1s)	~55.0	

TABLE I. (Continued)

Br(3d)	77.6	~71.8
Li(1s)	56.4	57.2
		54.8
$1a_1$	28.2	21.7 (VII)
1e	24.2	
$2a_1$	17.4	17.0 (VIII)
2e, $3a_1$	11.3	
4e, $4a_1$, a_2	5.8	5.7 (IX)

[a]The binding energies were referenced with respect to the edge of the valence band for Cl^- or Br^-.

[b]The binding energies were referenced with respect to the edge of the valence band for IO_4^-.

TABLE II. Core-level energies (eV) and chemical shifts of the products (in eV).

Sample	Product	Identification	$E_b(Cl(2p_{3/2}))$ or $E_b(Br(3p_{3/2}))$	ΔE_b Present work	ref.13	ref.14
$NaClO_3$		ClO_3^-	207.3	0	0	
	A	Cl_2^-	200.0	-7.3		
	B	Cl^-	198.9[a]	-8.4	-7.1	
	C	?	197.9	-9.4		
$LiClO_4$		ClO_4^-	209.5	0	0	
	G	ClO_3^-	207.0	-2.5	-2.4	
	H	ClO_2^-	204.7	-4.8	-4.7	
	I	Cl_2^-	199.9	-9.6		
	J	Cl^-	199.3[a]	-10.2	-9.5	
$LiBrO_3$		BrO_3^-	190.9(77.6)[b]	0(0)		(0)
	N	BrO_2^-	187.7(74.9)	-3.2(-2.7)		
	O	BrO^-	186.2(72.5)	-4.7(-5.1)		
	P	Br^-	184.2(70.4)	-6.7(-7.2)		(-5.9)

[a] The $Cl(2p_{3/2})$ energy of KCl was determined to be 198.7 eV.

[b] The values in the parentheses are for the $Br(3d)$ lines.

Figure Captions

Figure 1.   Spectral changes in the Cl(2p) region of $NaClO_3$ irradiated
with 1.4 keV electrons. The total dose is given in the
boxes in units of Coulomb/cm^2. The dashed lines show the
results of a least-squares spectral fitting procedure. The
product peak A is assigned to Cl_2^- and peaks B and C to Cl^-
species. "PB" means "photobleaching."

Figure 2.   Spectral changes in the O(1s) region of $NaClO_3$ with electron
irradiation. Peaks D and F are assigned to molecular oxygen
and Na_2O, respectively. See text for discussion regarding
peak E and the residual peak at the parent location in
part (b).

Figure 3.   Spectral changes in the valence-band region of irradiated
$NaClO_3$. The product peak I is assigned to O(2s) and the
peaks II and III are assigned to Cl(3s) and (3p),
respectively.

Figure 4.   Spectral changes in the Cl(2p) region of $LiClO_4$ exposed to
AlK_α X-rays for 24 hours. The product peak G is assigned
to the expected locations of further reduction products
(see Fig. 5).

Figure 5.   Spectral changes in the Cl(2p) region of $LiClO_4$ irradiated
with 1.4 keV electrons. The product peaks G, H, I, and J
are assigned to ClO_3^-, ClO_2^-, Cl_2^-, and Cl^-, respectively.
Note that after photobleaching two different oxyanions,
ClO_4^- and ClO_3^-, are regenerated in significant amounts.

Figure 6. Spectral changes in the O(1s) region of irradiated $LiClO_4$. The major product peaks K, L, and M are assigned to ClO_3^-, ClO_2^-, and Li_2O, respectively. Any other product such as O_2 that might be present is obscured in the spectra.

Figure 7. Spectral changes in the valence band region of irradiated $LiClO_4$. Product peaks IV, V, and VI are assigned to O(2s) and Cl(3s) and (3p), respectively (see Fig. 3).

Figure 8. Spectral changes in the Br(3p) region of $LiBrO_3$ irradiated with 1.4 eV electrons. The spectral fitting indicates the presence of at least three products, N, O, and P assigned as BrO_2^-, BrO^-, and Br^-, in part (b).

Figure 9. Spectral changes in the O(1s) region of irradiated $LiBrO_3$. Product peaks Q and R are assigned to BrO_2^- and Li_2O respectively.

Figure 10. Spectral changes in the valence band region of irradiated $LiBrO_3$. Product peaks VII, VIII, and IX are assigned to O(2s), Br(4s) and O(2p) + Br(4p), respectively, of Li_2O and Br^-.

Figure 11. Relative yields of X_2^- + X^- and Li_2O in irradiated $LiClO_4$ and $LiBrO_3$ as a function of total radiation dose (Coulomb/cm^2 at 1.4 keV). The yields were estimated from the peak intensities of the O(1s) line and Cl(2p) or Br(3p) line. Open circles and squares denote the photobleached samples.

26
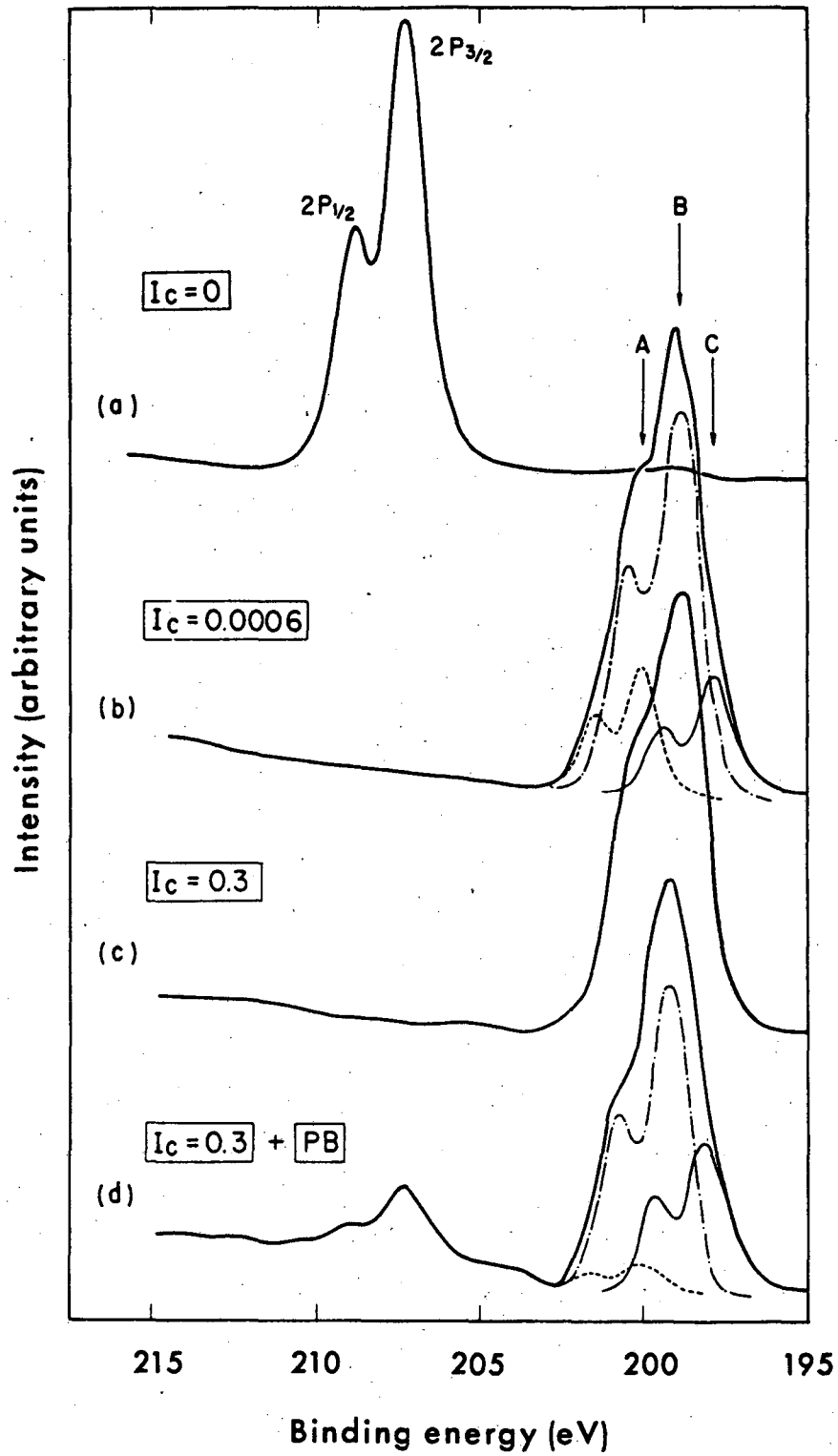
Figure 1
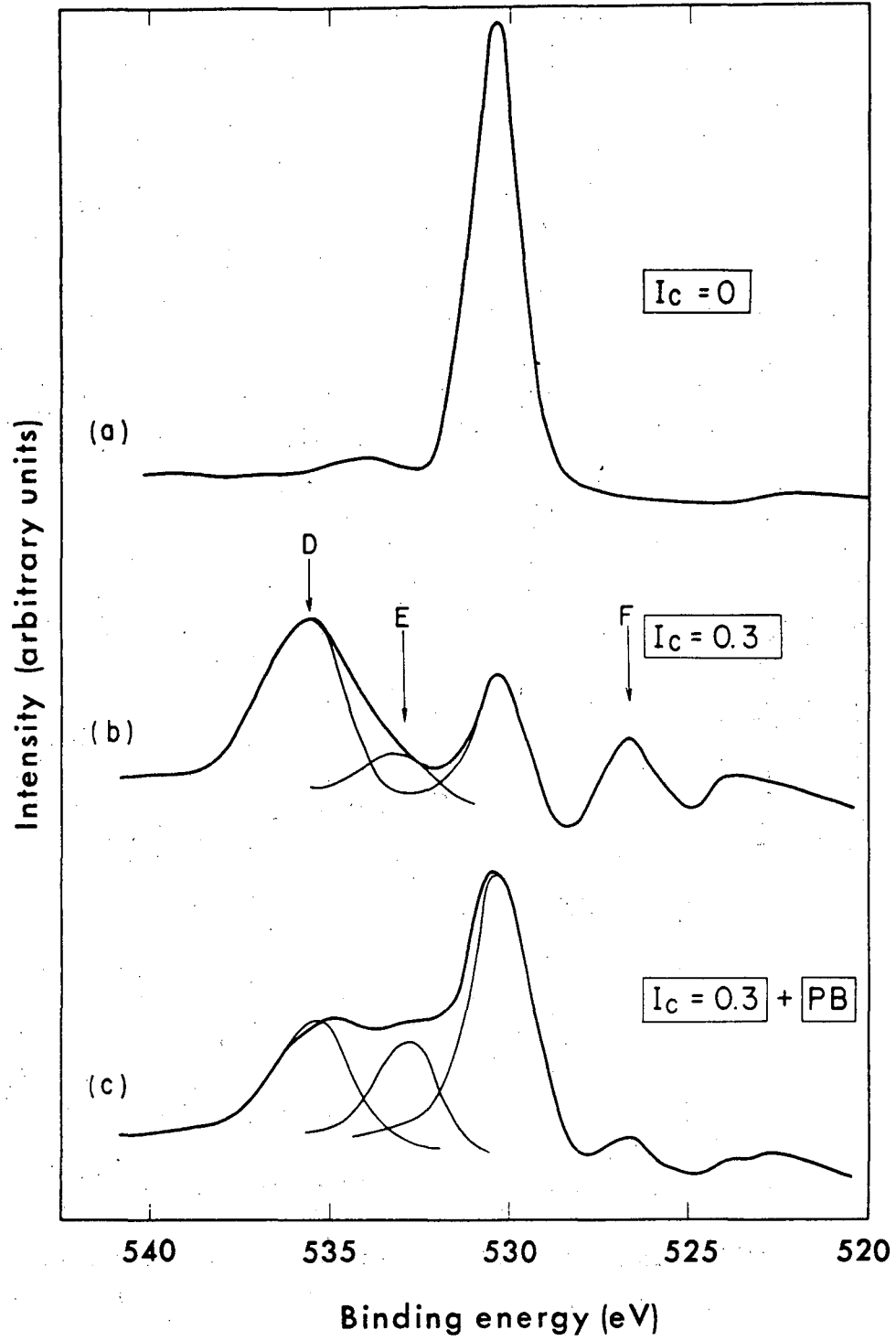
XBL 789-1740

XBL 789-1738

Figure 2
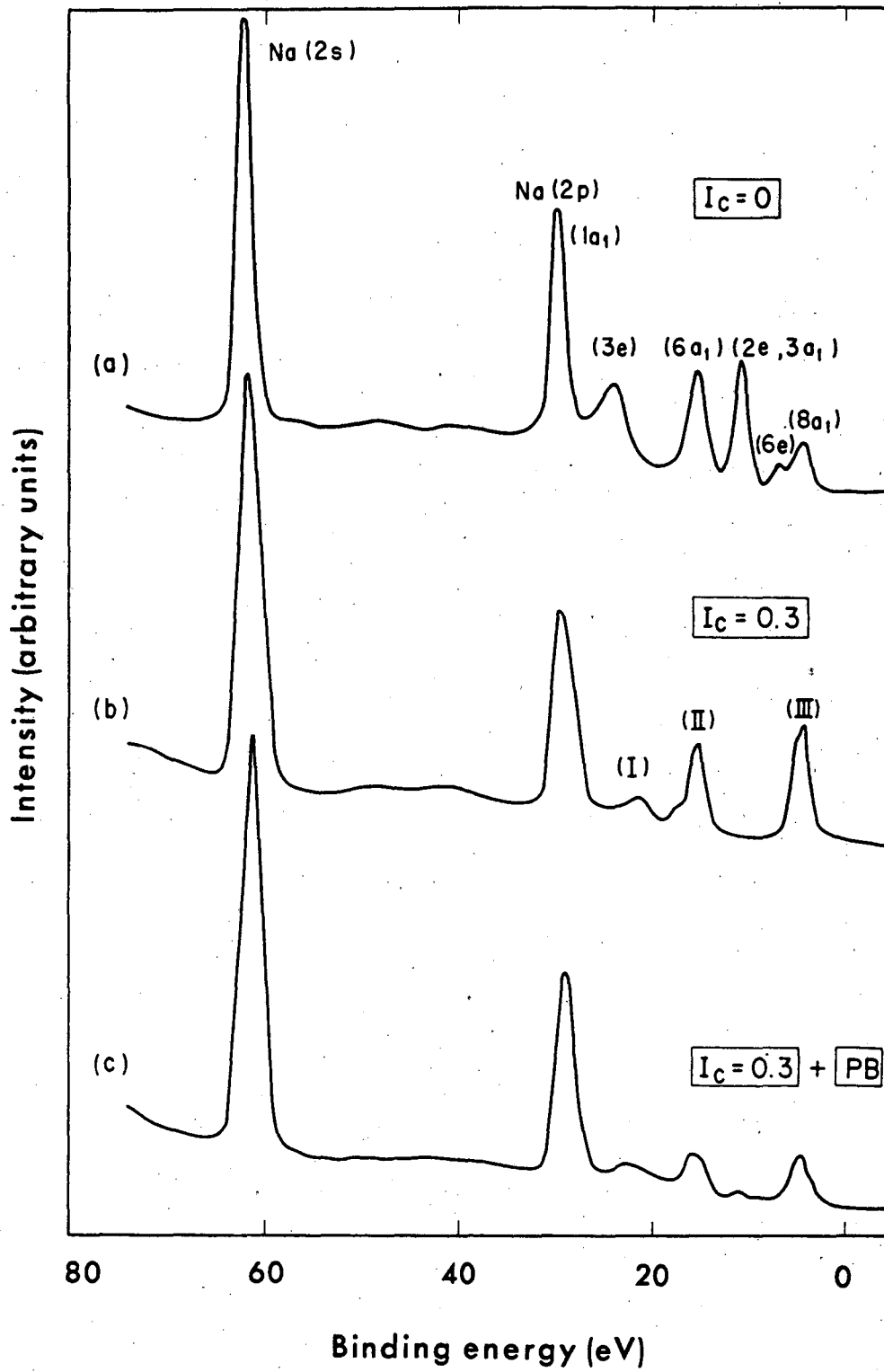
Figure 3
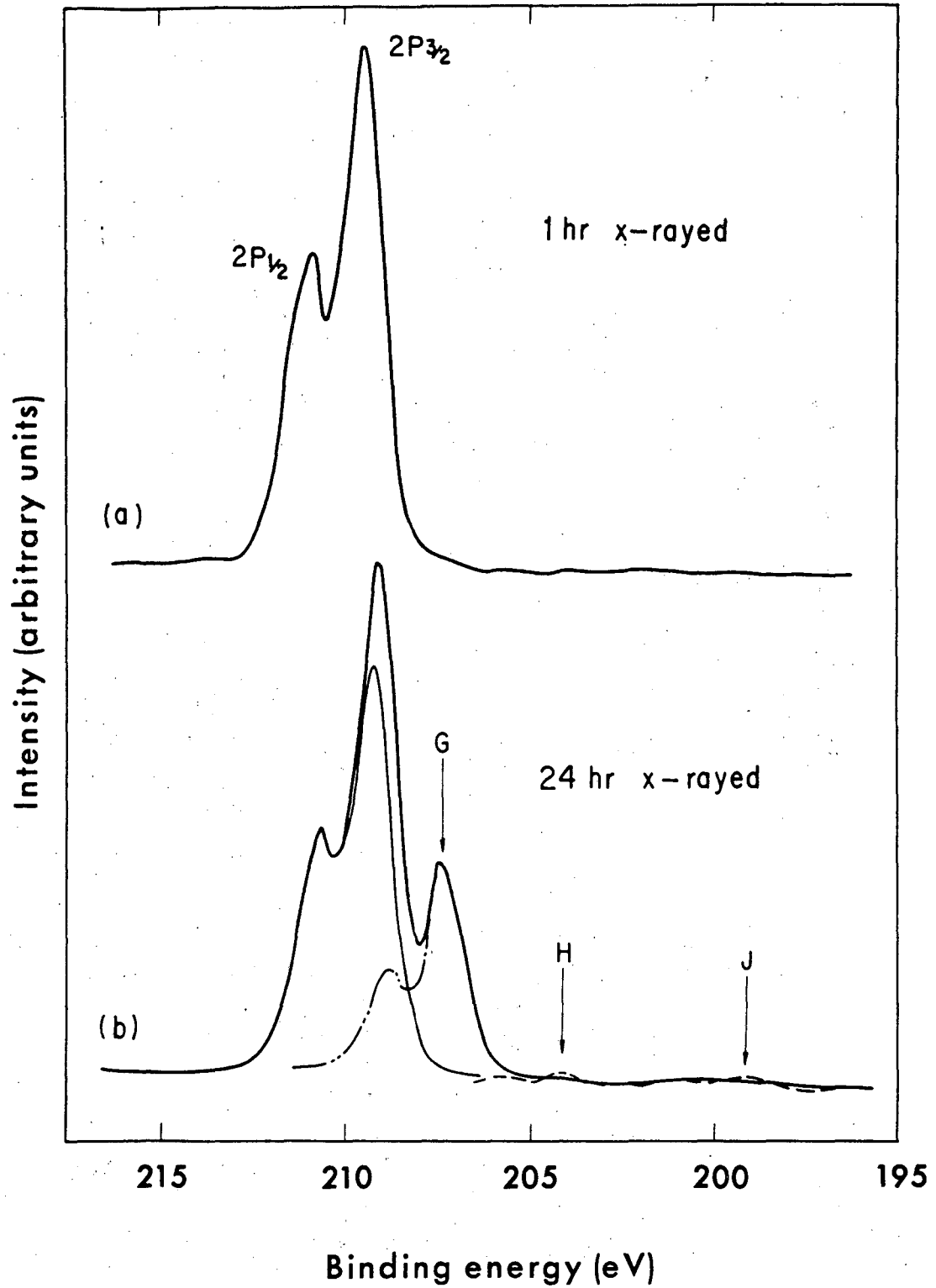
XBL 789-1739
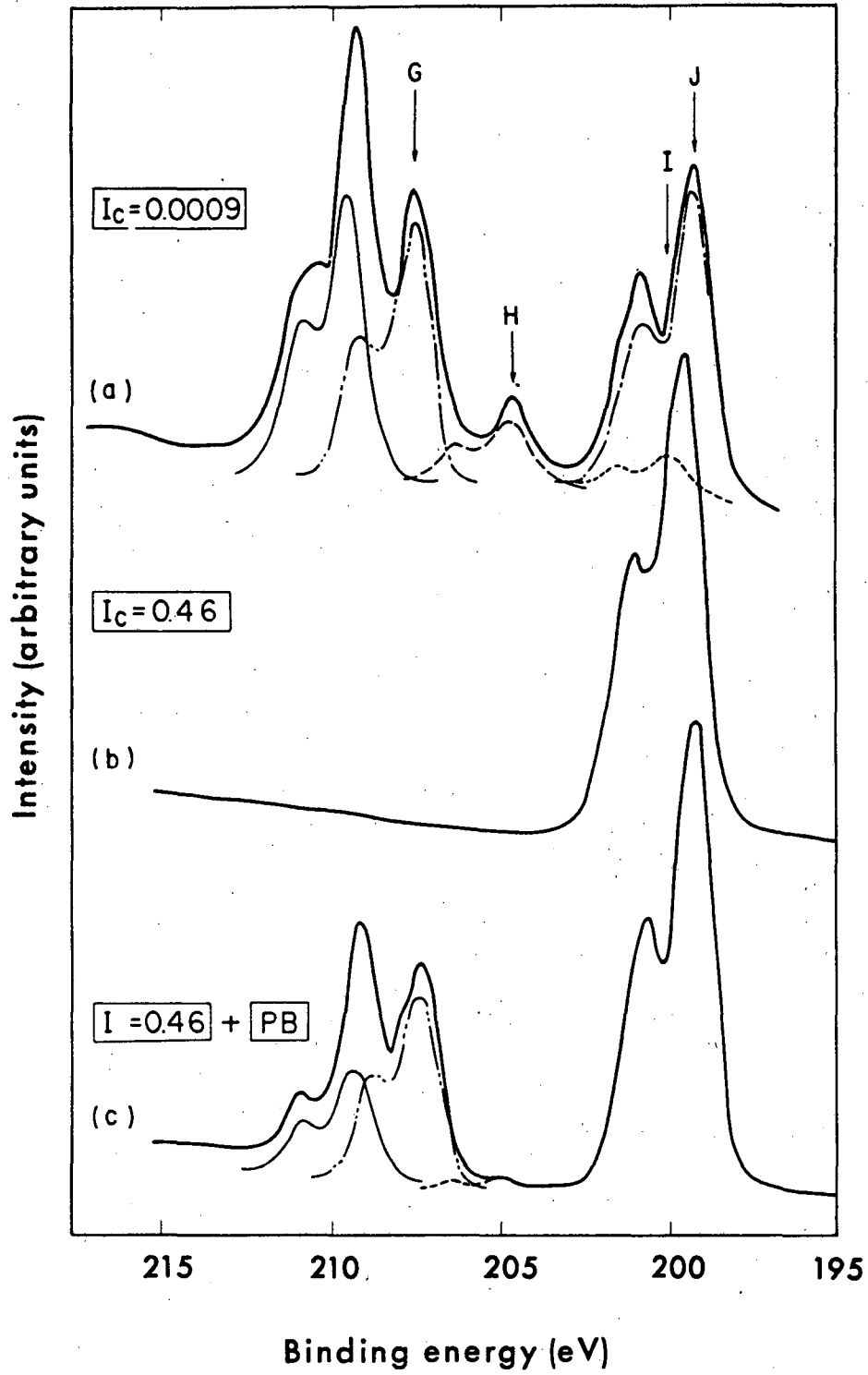
Figure 4

Figure 5
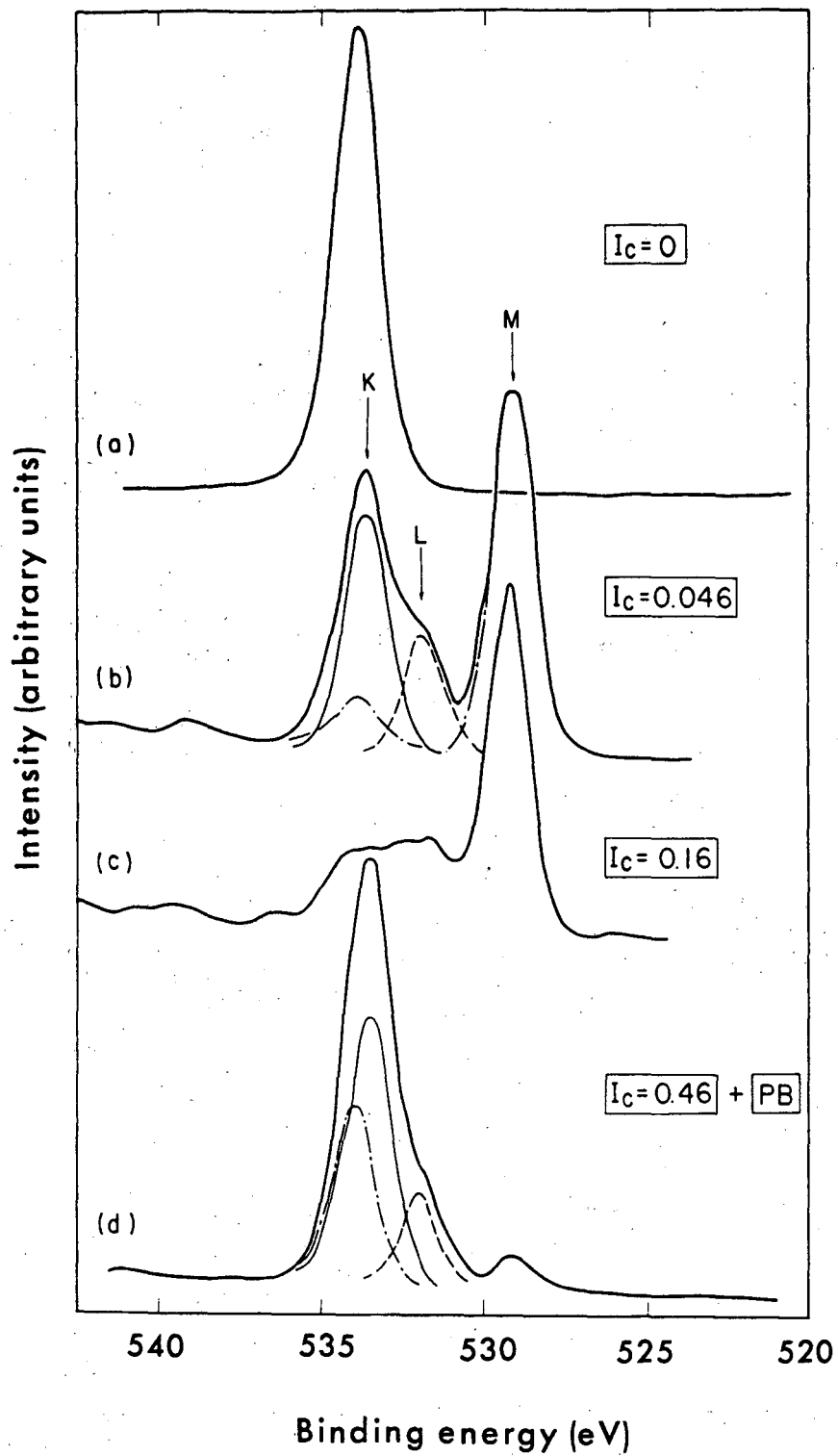
XBL 789-1743

XBL 789-1737

Figure 6
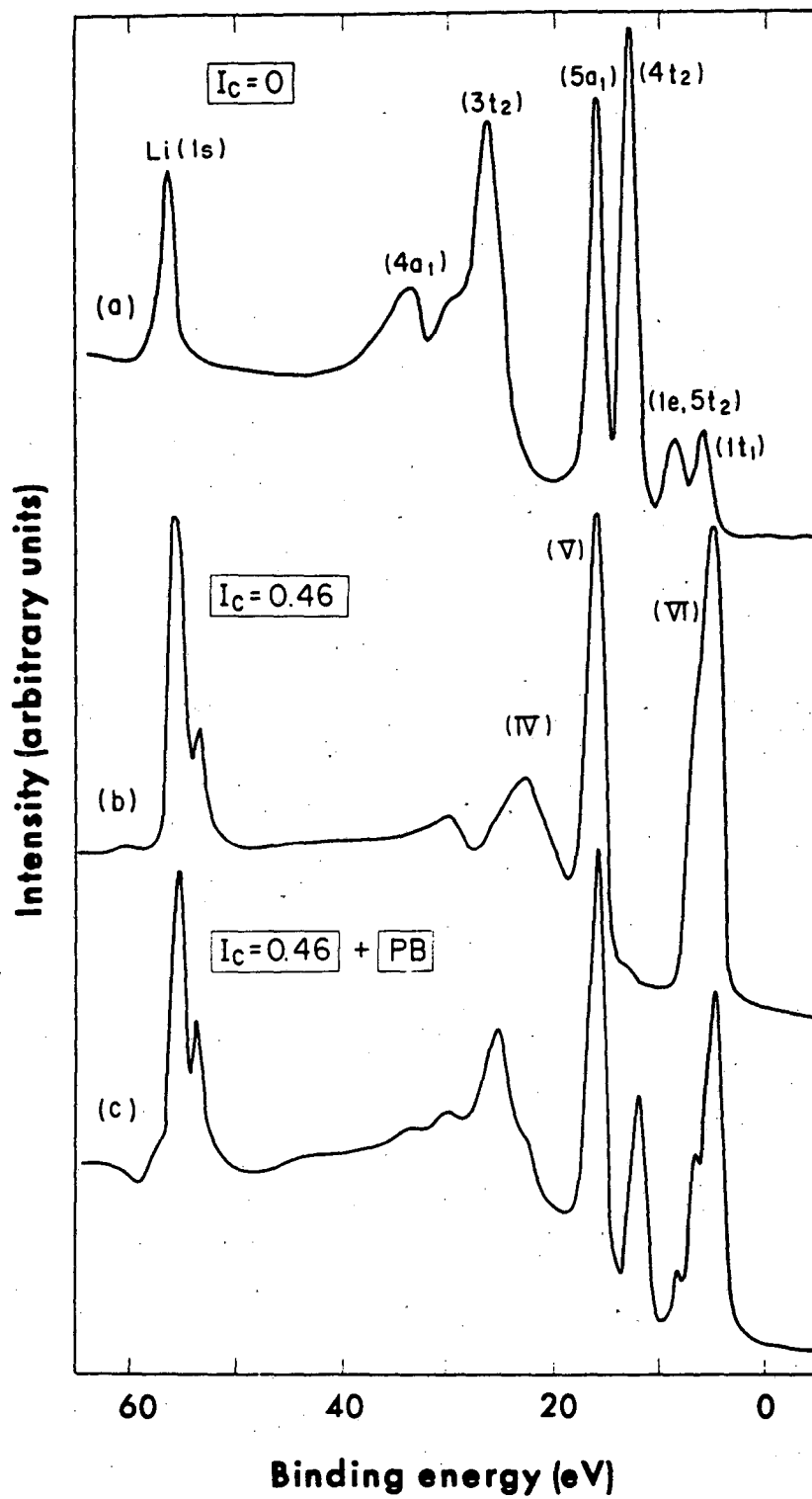
Figure 7

XBL 789-1744

Figure 8

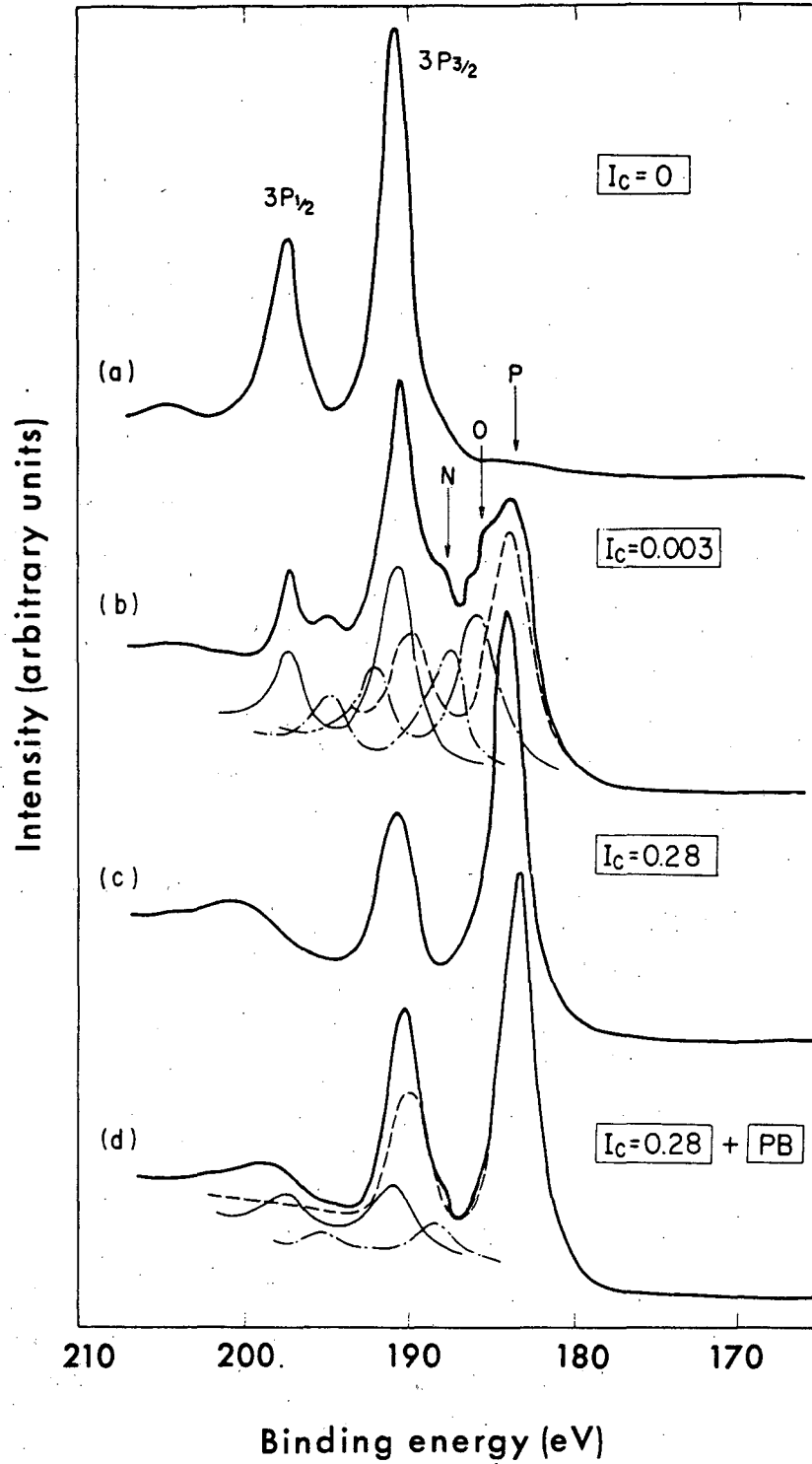XBL 789-1742A

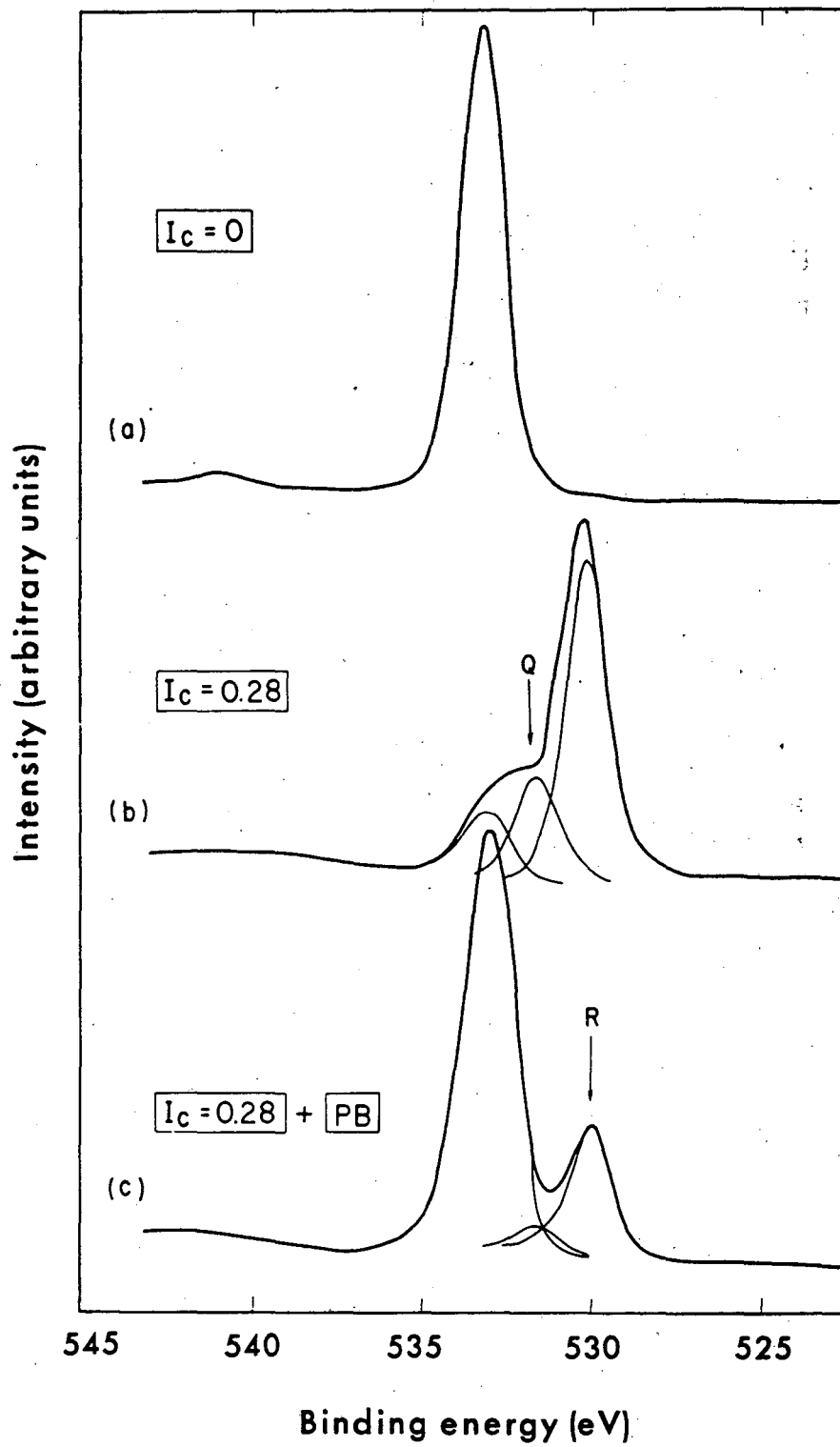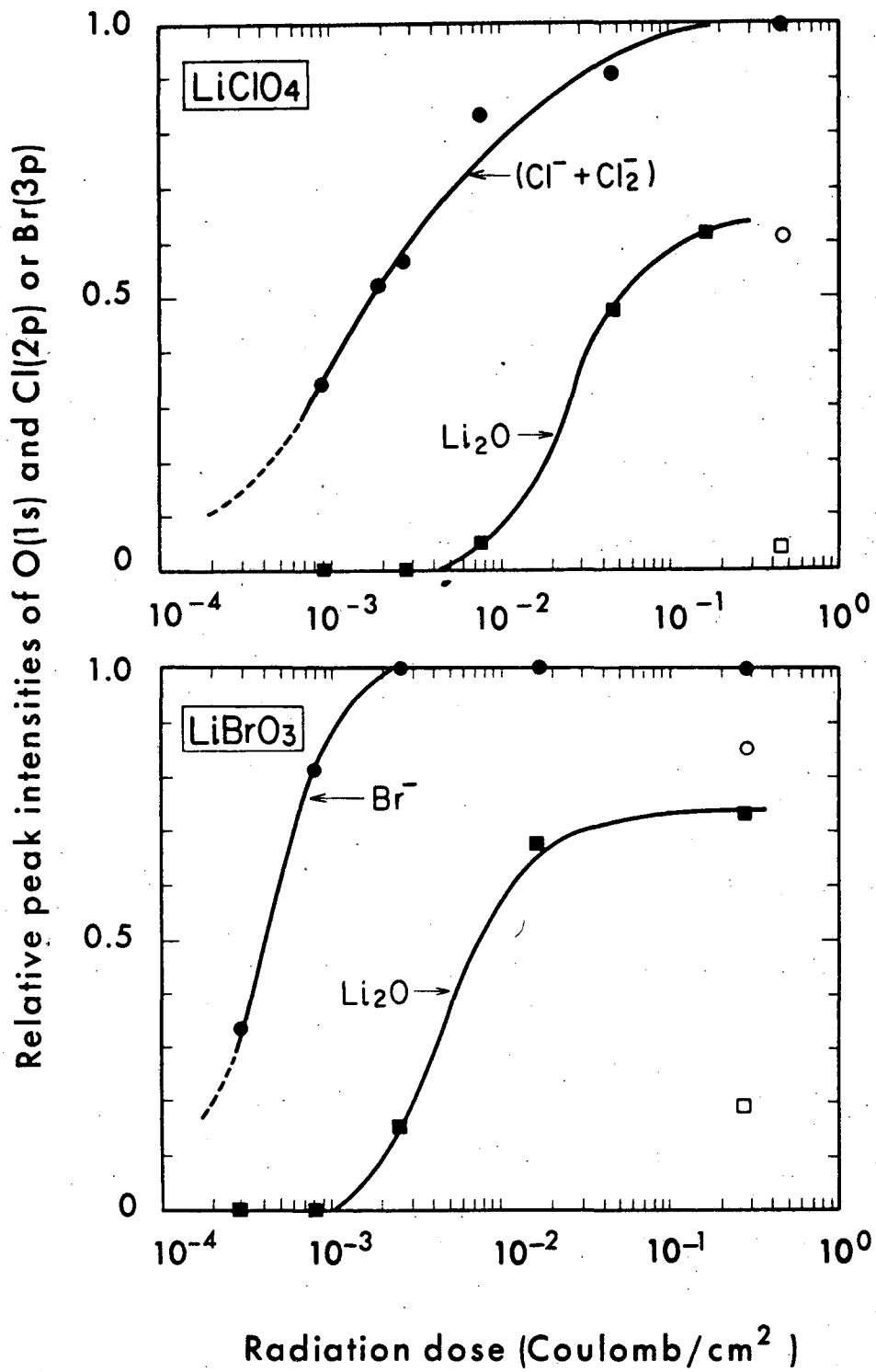XBL 789-1736

Figure 9
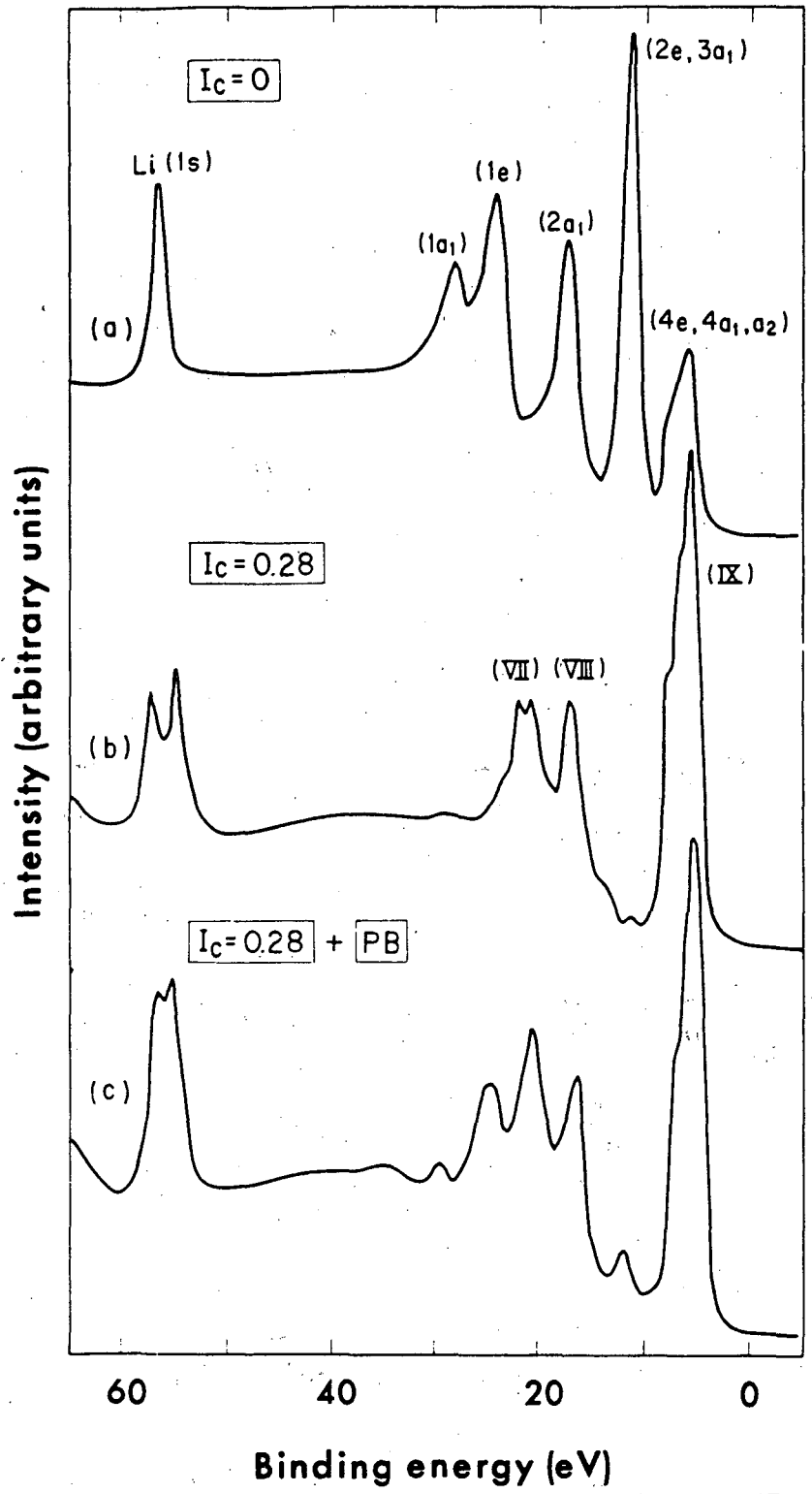
XBL 789-1745

Figure 10

XBL 789-1735

Figure 11